J. Plasma Physics (2000), *vol.* 64, *part* 2, *pp.* 131–153. Printed in the United Kingdom

© 2000 Cambridge University Press

The Boltzmann relation in electronegative plasmas: When is it permissible to use it?

R. N. FRANKLIN and J. SNELL

Oxford Research Unit, The Open University, Foxcombe Hall, Boars Hill, Oxford OX1 5HR, UK

(Received 16 December 1999 and in revised form 5 May 2000)

Abstract. This paper reports the results of computations to obtain the spatial distributions of the charged particles in a bounded active plasma dominated by negative ions. Using the fluid model with a constant collision frequency for electrons, positive ions and negative ions the cases of both detachment-dominated gases (such as oxygen) and recombination-dominated gases (such as chlorine) are examined. It is concluded that it is valid to use a Boltzmann relation $n_e = n_{e0}\exp(eV/kT)$ for the electrons of density n_e, where the temperature T is approximately the electron temperature T_e, and that the density n_n of the negative ions at low pressures obeys $n_n = n_{n0}\exp(eV/kT_n)$, where T_n is the negative-ion temperature. However, at high pressure in detachment-dominated gases where the ratio of negative-ion density to electron density is constant and greater than unity, and when the attachment rate is larger than the ionization rate, the negative ions are distributed with the same effective temperature as the electrons. In all other cases there is *no* simple relationship. Thus to put $n_n/n_e = \text{const}$, $n_n = n_{e0}\exp(eV/kT_e)$ and $n_n = n_{n0}\exp(eV/kT_n)$ simultaneously is mathematically inconsistent and physically unsound. Accordingly, expressions deduced for ambipolar diffusion coefficients based on these assumptions have no validity. The correct expressions for the situation where $n_n/n_e = \text{const}$ are obtained without invoking a Boltzmann relation for the negative ions.

1. Introduction

An assumption that is frequently made in plasma physics is that when the plasma is contained in a potential well that confines the negative particles, it accelerates the positive ones so that the fluxes of particles of opposite sign are equal throughout the volume all the way to the boundary wall. In the absence of negative ions, this gives rise to the concept of ambipolar diffusion at higher pressure (Schottky 1924).

In situations where there are a significant number of negative ions and the plasma is essentially collisionless, it *is* permissible to set $n_e = n_{e0}\exp(-\phi)$, where n_e is the electron density, n_{e0} the central electron density and $\phi = -eV/kT_e$ (where V is the electrostatic potential and T_e the electron temperature) measured relative to the potential at the centre (k is Boltzmann's constant and e the electronic charge) *and* to set $n_n = n_{n0}\exp(-\varepsilon_n\phi)$, where n_n is the negative ion density and $\varepsilon_n = T_e/T_n$ (where T_n is the negative-ion

https://doi.org/10.1017/S0022377800008576 Published online by Cambridge University Press

temperature). This follows from their respective equations of motion to the walls under the potential gradient.

The purpose of this paper is to examine the range of validity of using $n_n = n_{n0}\exp(-\varepsilon_n\phi)$ in electronegative plasmas, be they determined by detachment (e.g. O_2) or recombination (e.g. Cl_2) as has been done in conditions where the diffusion was ambipolar by Thompson (1959), reproduced by Massey (1976), and again in more recent work (e.g. Lieberman and Lichtenberg (1994). The use of $n_e \approx n_{e0}\exp(-\phi)$ is not at issue, since Kaganovich and Tsendin (1993) showed that

$$n_e = n_{e0}\exp\left(-\frac{\phi}{f}\right),$$

where

$$f = \frac{1+\alpha\dfrac{D_n}{D_e}-(\alpha+1)\dfrac{D_p}{D_e}}{1+\alpha\dfrac{\mu_n}{\mu_e}+(\alpha+1)\dfrac{\mu_p}{\mu_e}}$$

and the Ds are diffusion coefficients, the μs mobilities and α the ratio of negative ion density to electron density; the subscripts e, p and n refer to electrons, positive ions and negative ions respectively. α is assumed to be slowly varying in the region to which it is applied. Now typically μ_n/μ_e, $\mu_p/\mu_e < 10^{-2}$ and D_n/D_e, $D_p/D_e < 10^{-4}$, so that α must be greater than 100 before there is any *significant* departure from conventional Boltzmann equilibrium for the electrons. But if $n_n \approx \alpha n_e$ then $(\nabla n_n)/n_n = (\nabla n_e)/n_e$, and thus $n_n \approx n_{n0}\exp(-\phi)$, not $n_{n0}\exp(-\varepsilon_n\phi)$.

The method that we shall use is to write down and integrate the relevant equations for electrons, positive ions and negative ions in a form that allows the possibility of describing the transition from collisionless plasmas to collisional using the *same* set of equations and simply varying the normalized ion collision frequencies $\delta_{p,n} \equiv \nu_{p,n}/Z$, where ν_p and ν_n are the collision frequencies for momentum transfer and Z is the ionization rate. We shall work in plane geometry, i.e. with parallel bounding walls, for simplicity (but similar conclusions apply in the cylindrical case), and always in the quasineutral or plasma approximation. This use of a constant collision frequency is a simplification of the true situation at intermediate pressures, where the mean free path is more closely constant, but it gives the recognized results at both limits, namely $\delta_p \to 0$ and $\delta_p \to \infty$, and for that reason is a suitable bridge. This was first demonstrated for electropositive gases by Forrest and Franklin (1966), who described the transition from the collisionless Tonks–Langmuir description to the Schottky one by such a variation of δ_p.

Obtaining a measure of the difference between the two competing expressions is not a simple matter, since $n_n = n_{n0}$ at $x = 0$, and at higher pressures, $n_n = 0$ at the wall $x = x_w$ in any case; for that reason, we have adopted the approach of calculating two factors. The first is

$$\varepsilon_{\text{eff}} = \frac{-1}{\phi}\ln\left(\frac{n_n}{n_{n0}}\right)$$

and the second

$$\varepsilon^l_{\text{eff}} = \frac{-1}{\Delta\phi}\ln\left[\frac{n_n(x+\Delta x)}{n_n(x)}\right] \quad \text{as} \quad \Delta x \to 0,$$

https://doi.org/10.1017/S0022377800008576 Published online by Cambridge University Press

where $\Delta\phi = \phi(x+\Delta x)-\phi(x)$. This approach allows the possibility of treating both structured and unstructured discharges in the same way. $\varepsilon^{l}_{\text{eff}}$ is a *local* measure and ε_{eff} an overall one.

The fact that such discharges may be structured, i.e. consist of an ion–ion core surrounded by an electron–ion plasma, was pointed out by Franklin (1976) in his discussion of the work of Edgley (1975), and occurs again in the work of Ferreira et al. (1988). Further theoretical examination of structured discharges has been undertaken by Tsendin (1989), Daniels et al. (1990) Franklin et al. (1993) and Franklin and Snell (1994). For simplicity, we shall take $\mu_n = \mu_p = \mu_i$, $\nu_n = \nu_p = \nu_i$ and $T_n = T_p = T_i$ in order to reduce the number of parameters. In typical situations, they may differ by a factor of up to three, but not by an order of magnitude, and $\mu_e \gg \mu_i$ and $T_e \gg T_i$. We shall also give the spatial variation of ε_{eff} in the transition region to indicate whether or not the concept of an ε_{eff} is meaningful. In this way, we seek to map out the transition so far as negative ions are concerned from $n_n = n_{n0}\exp(-\varepsilon_n\phi)$ at low pressure to $n_n \approx n_{n0}\exp(-\phi)$ at high pressure, indicating the parameters that determine the transition.

We believe that this is the first approach taking the basic equations for the particles and using them to address what is a fundamental issue in the treatment of electronegative plasmas.

2. Basic equations

We shall assume initially that the discharge is one in which the negative ions are formed by attachment and lost by detachment, so that the continuity or generation and loss of equations for the ions are

$$\nabla\cdot(n_p\,\mathbf{v}_p) = Zn_e, \tag{1}$$

$$\nabla\cdot(n_n\,\mathbf{v}_n) = An_e - Dn_n, \tag{2}$$

where Z is the ionization rate, A the attachment rate and D the detachment rate. The continuity equation for electrons $\nabla\cdot(n_e\,\mathbf{v}_e) = Zn_e - An_e + Dn_n$ is the difference between (1) and (2).

The equations of motion, or conservation of momentum, are

$$\nabla\cdot(n_q\,\mathbf{v}_q\,\mathbf{v}_q) + \frac{kT_q}{m_q}\nabla n_q + \nu_q\,n_q\,\mathbf{v}_q + \frac{q_q}{m_q}n_q\,\nabla V = 0, \tag{3a, b, c}$$

where $q = e,p$ and n for electrons, positive ions and negative ions respectively, and $\mathbf{v}_q$ are the particle velocities, m_q the particle masses and ν_q the collision frequencies for momentum transfer.

Consistent with the fact that $m_e \ll m_p$, m_n, and in the light of the discussion in Sec. 1, we set the first term of (3a) to zero because this eliminates m_e/m_p as a parameter, and after normalizing all quantities by

$$E = \frac{n_e}{n_{e0}}, \qquad N = \frac{n_n}{n_{e0}}, \qquad I = \frac{n_p}{n_{e0}},$$

$$\delta_n = \frac{\nu_n}{Z}, \qquad \delta_p = \frac{\nu_p}{Z}, \qquad P = \frac{A}{Z}, \qquad Q = \frac{D}{Z},$$

https://doi.org/10.1017/S0022377800008576 Published online by Cambridge University Press

$$U = \frac{\mathbf{v}_p}{c_s}, \qquad W = \frac{\mathbf{v}_n}{c_s}, \qquad c_s^2 = \frac{kT_e}{m_p}, \qquad X = \frac{xZ}{c_s},$$

$$\varepsilon_p = \frac{T_e}{T_p}, \qquad \varepsilon_n = \frac{T_e}{T_n}, \qquad \delta_e = \frac{m_e}{m_p}\frac{\nu_e}{Z},$$

we have

$$\frac{dE}{dX} + E\frac{d\phi}{dX} + \delta_e(IU - NW) = 0, \tag{4}$$

$$\frac{d}{dX}(IU) = E, \tag{5}$$

$$\frac{d}{dX}(IU^2) + \frac{1}{\varepsilon_p}\frac{dI}{dX} + \delta_p IU - I\frac{d\phi}{dX} = 0, \tag{6}$$

$$\frac{d}{dX}(NW) = PE - QN, \tag{7}$$

$$\frac{d}{dX}(NW^2) + \frac{1}{\varepsilon_n}\frac{dN}{dX} + \delta_n NW + N\frac{d\phi}{dX} = 0. \tag{8}$$

Quasineutrality is expressed as

$$I = N + E. \tag{9}$$

To obtain (4), we have used (3a) with $m_e = 0$ and the fact that $n_e \mathbf{v}_e = n_p \mathbf{v}_p - n_n \mathbf{v}_n$. The ionization rate is strongly dependent on T_e, the attachment and detachment rates are generally constant, and their spatial variations are small.

Eliminating dU/dX between (5) and (6) and dW/dX between (7) and (8) gives

$$\left(U^2 - \frac{1}{\varepsilon_p}\right)\frac{dI}{dX} + I\frac{d\phi}{dX} = 2EU + \delta_p IU, \tag{10}$$

$$\left(W^2 - \frac{1}{\varepsilon_n}\right)\frac{dN}{dX} - N\frac{d\phi}{dX} = 2(PE - QN)\,W + \delta_n NW, \tag{11}$$

and (4) can be written as,

$$\frac{dI}{dX} - \frac{dN}{dX} + E\frac{d\phi}{dX} = \delta_e(NW - IU). \tag{12}$$

Thus

$$\begin{pmatrix} U^2 - \frac{1}{\varepsilon_p} & I & 0 \\ 0 & -N & W^2 - \frac{1}{\varepsilon_n} \\ 1 & E & -1 \end{pmatrix} \begin{pmatrix} \frac{dI}{dX} \\ \frac{d\phi}{dX} \\ \frac{dN}{dX} \end{pmatrix} = \begin{pmatrix} 2EU + \delta_p IU \\ 2(PE - QN)\,W + \delta_n NW \\ \delta_e(NW - IU) \end{pmatrix}. \tag{13}$$

https://doi.org/10.1017/S0022377800008576 Published online by Cambridge University Press

The boundary at low pressure occurs where the determinant Δ of the matrix goes to zero or,

$$\Delta = N\left(U^2-\frac{1}{\varepsilon_p}\right)-E\left(U^2-\frac{1}{\varepsilon_p}\right)\left(W^2-\frac{1}{\varepsilon_n}\right)+I\left(W^2-\frac{1}{\varepsilon_n}\right)=0; \tag{14}$$

when $W=0$, this can be written as

$$U^2=\frac{1}{\varepsilon_p}+\frac{I}{E+\varepsilon_n N}, \tag{15}$$

and this coincides with the results of other workers (e.g. Riemann 1995; Valentini and Herrmann 1996), and is a generalized Bohm criterion. The value of X at $x=x_w$ is denoted by X_W.

However I, N and E are also required to be non-negative, and this condition may be the determining one at higher pressures.

It should also be noted that (5) and (7) are auxiliary to (13), and *their* importance is brought out later in discussion of the electron and ion fluxes.

3. Computing the solutions

The set of three coupled first-order differential equations can be solved by standard methods by integrating from the centre $X=0$, where

$$E=1, \quad N=N_0, \quad I=N_0+1,$$

$$\frac{dE}{dX}=\frac{dI}{dX}=\frac{dN}{dX}=0,$$

$$U=0, \quad W=0, \quad \phi=0, \quad \frac{d\phi}{dX}=0,$$

with the other quantities ε_p, ε_n, δ_p, δ_n, P and Q as parameters. In order to concentrate on the physics of the problem as indicated in Sec. 1, we set $\varepsilon_p=\varepsilon_n=\varepsilon_i$ and $\delta_p=\delta_n=\delta_i$, so that the number of parameters, including N_0, is reduced to five.

The method used was a simple extension of that described in Appendix 1 of Franklin and Snell (1999a), where we had (13) with $\delta_e=\delta_m$ and $\delta_p=\delta_n=0$, so we shall not repeat those details here.

A wide range of parameters was examined, $0\leqslant N_0\leqslant 30$, $10\leqslant\varepsilon_i\leqslant 100$, $0.01\leqslant\delta_i\leqslant 1000$, $0.3<Q<3$, but in order to focus on the particular aspects that we are concerned with, we concentrate on $N_0=30$, $\varepsilon_i=100$ and $Q=0.3$.

Figure 1 shows the variation of the ratio of negative-ion density to electron density across the plasma for $\delta_i=0.01$, 1, 100 and 1000 for $\varepsilon_i=100$, indicating how $\alpha=$ const becomes a better approximation as δ_i increases. Figure 2 gives the spatial variation of ε_{eff} for values of $\delta_i=0.01$, 0.1, 1, 10, 100 and 300, and again $\varepsilon_i=100$, showing that ε_{eff} is relatively constant across most of the plasma and that its value is much less than ε_i for $\delta_i\geqslant 1$ and that $\varepsilon_{\text{eff}}\approx\varepsilon_i$ holds only for $\delta_p\leqslant 0.01$. One feature that is noteworthy is the increase in ε_{eff} (and $\varepsilon^l_{\text{eff}}$) near the wall. This is not surprising, since the negative-ion flux is zero at the wall and therefore, from (8), $n_n\sim\exp(-\varepsilon_i\phi)$ locally and so $\varepsilon^l_{\text{eff}}$ rises to ε_i at the wall.

https://doi.org/10.1017/S0022377800008576 Published online by Cambridge University Press

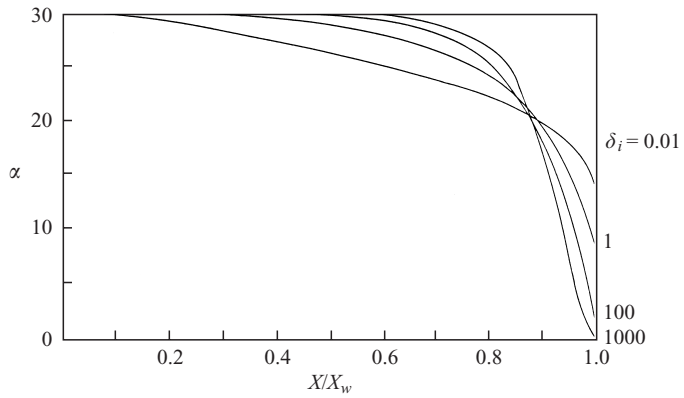


Figure 1. The variation of the negative-ion/electron density ratio α across an attachment–detachment plasma at high electronegativity, $\alpha_0 = 30$, for different values of $\delta_i = \nu_i/Z = 0.01$, 1, 100 and 1000, where $\nu_i = \nu_p$ is the positive-ion collision frequency and Z the ionization rate, as $\delta_i \to \infty$, $\alpha \to \alpha_0$, for all X. $\varepsilon_n \equiv T_e/T_n = 100$ and $Q = D/Z = 0.3$, D being the detachment rate.

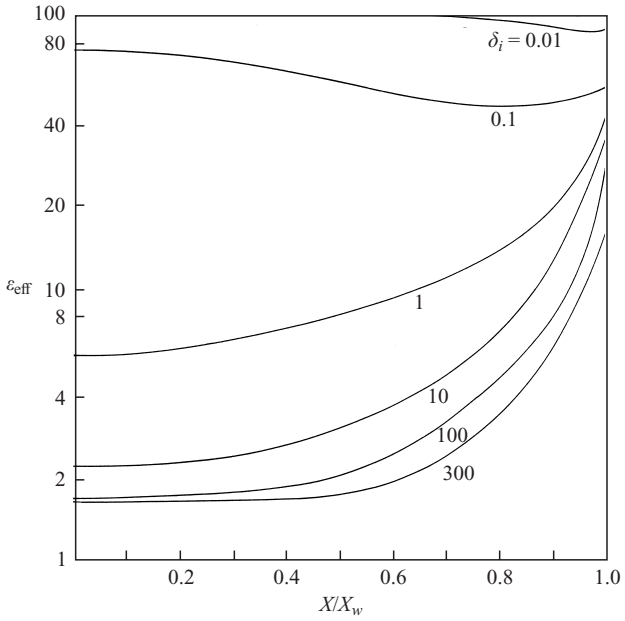


Figure 2. The variation of ε_{eff}, the effective electron temperature to negative-ion temperature ratio, given by $\varepsilon_{\text{eff}} = (1/\phi)\ln(N_0/N)$, as a function of δ_i for $\delta_i = 0.01$, 0.1, 1, 10, 100 and 300. $\varepsilon_{\text{eff}} \approx 100$ for small δ_i, but for $\delta_i > 1$, $\varepsilon_{\text{eff}} = O(1)$. $\varepsilon_n = 100$, $Q = 0.3$, $N_0 = 30$, $P \approx 8$.

Appendix C gives a proof of why this should be so. However, it is important to recognize that in the region where the Boltzmann relation applies for the negative ions with their own temperature, their density is going rapidly to zero and is less than that of the electrons, so that $n_n/n_e \approx \alpha$ no longer applies. We shall return to this point in Sec. 4. Figure 3 displays the central value of $\varepsilon_{\text{eff}} \equiv \varepsilon^l_{\text{eff}}$ as a function of δ_i, indicating again that $n_n \sim n_{n0}\exp(-\varepsilon_i\phi)$ holds only for $\delta_i < 0.1$.

https://doi.org/10.1017/S0022377800008576 Published online by Cambridge University Press

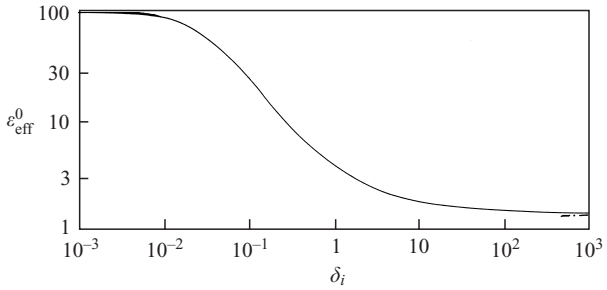


Figure 3. The variation of $\varepsilon^0_{\rm eff}$, the central value of $\varepsilon_{\rm eff}$ with δ_i for the same parameters as in Fig. 2. The asymptote corresponds to $N \propto E$ at high pressures.

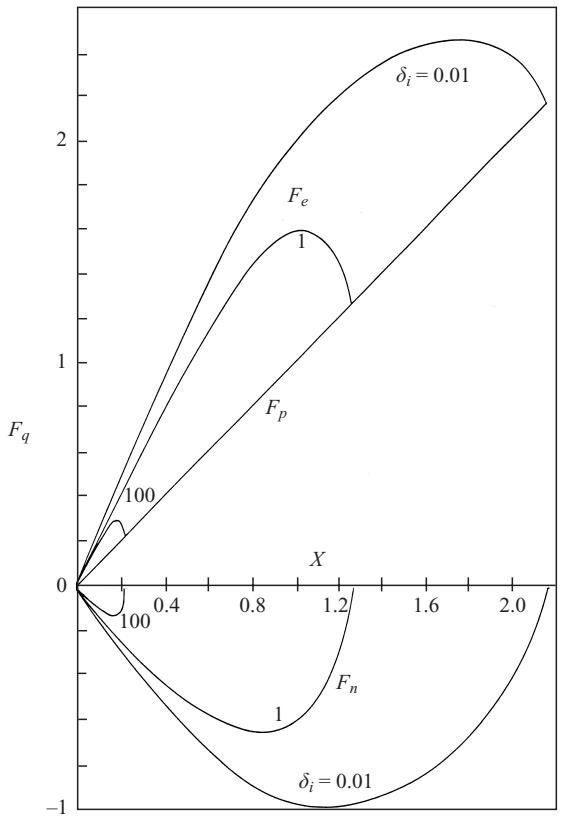


Figure 4. The charged-particle fluxes as functions of position for $\delta_i = 0.01$, 1 and 100. Note that the negative-ion flux is always negative and the normalized positive-ion flux is given to high accuracy by X.

Figure 4 shows the normalized fluxes of each type of particle ($F_p = IU$ for positive ions, $F_n = NW$ for negative ions and $F_e = IU - NW$ for electrons) for $\delta_i = 0.01, 1$ and 100; the curves are similar over the whole range. It is evident that throughout the range the fluxes are comparable in magnitude and that the normalized positive-ion flux is very closely equal to X. Thus the validity of any relation obtained by setting one flux or another to zero needs to be carefully examined.

https://doi.org/10.1017/S0022377800008576 Published online by Cambridge University Press

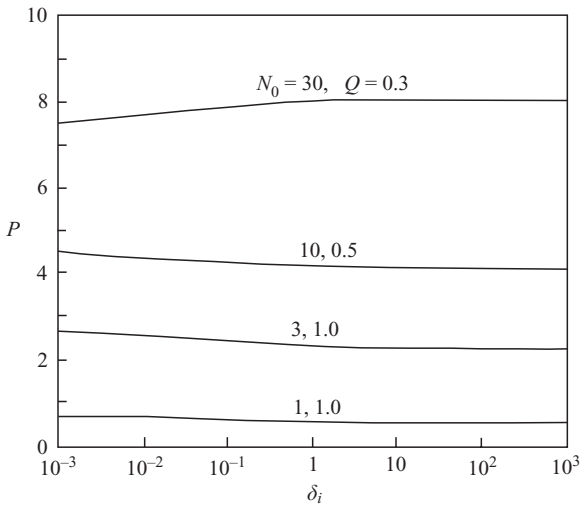


Figure 5. The value of P found by computation to satisfy the boundary conditions for different values of N_0 and Q as a function of δ_i. The asymptotic value for large δ_i agrees with (B 6) to approximately 0.1 % for $N_0 \geqslant 3$.

Since the method of solution involved varying P for fixed N_0, Q, δ_i and ε_i in order to meet the boundary conditions, it is appropriate to show P as a function of δ_i. Figure 5 shows the variation of P with δ_i over the range $0.001 < \delta_i < 1000$ for fixed values of N_0 and Q. It is remarkable how little P varies with δ_i; indeed, for $\delta_i \geqslant 1$, it is within 0.1 % of the value given by (B 6) (see Appendix B), which is a simple generalization of equation (33) of Ferreira et al. (1988) obtained in the high-pressure mobility–diffusion limit.

3.1. Solutions near $X = 0$

In order to start the integration, one needs values near the origin, since some quantities are zero at $X = 0$.

It is readily seen that E, N and I are even functions of X, as is ϕ, while U and W are odd. Expanding in power series

$$E = 1 - e_2 X^2 + \dots, N = N_0 - n_2 X^2 + \dots,$$
$$I = N_0 + 1 - (n_2 + e_2) X^2 + \dots,$$
$$\phi = f_2 X^2 + \dots, \quad U = u_1 X + \dots,$$
$$W = w_1 X + \dots,$$

from (5) we find

$$(N_0 + 1)\, u_1 = 1, \tag{5′}$$

and from (7) we find

$$N_0\, w_1 = P - Q N_0, \tag{7′}$$

while (6) gives

$$2(N_0 + 1)\, u_1^2 - \frac{2(n_2 + e_2)}{\varepsilon_p} + \delta_p (N_0 + 1)\, u_1 - 2(N_0 + 1) f_2 = 0, \tag{6′}$$

(8) gives

$$2 N_0\, w_1^2 - \frac{2 n_2}{\varepsilon_n} + \delta_n N_0\, w_1 + 2 N_0 f_2 = 0, \tag{8′}$$

https://doi.org/10.1017/S0022377800008576 Published online by Cambridge University Press

and (4) gives

$$-2e_3+\delta_e[(N_0+1)\,u_1-N_0\,w_1]+2f_2=0. \tag{4′}$$

Using (5′) and (7′) to eliminate u_1 and w_1 in (6′), (8′) and (4′) gives three linear equations in e_2, n_2 and f_2, which can be solved to enable the integration to begin and proceed from small X outwards.

Furthermore, for large δ_p, N_0 and ε_i, consistency requires

$$\frac{1}{P-QN_0}=\frac{-(N_0+1)}{N_0}$$

or

$$N_0+P(N_0+1)=QN_0(N_0+1), \tag{16}$$

so this relationship, first written down by Ferreira et al. (1988), is the limiting case at high pressure and high negative-ion density in the current work.

Equally, when δ_p, $\delta_e\to 0$ and $P\to 0$, $Q\to 0$ and $\varepsilon_p\to\infty$, we recover the expressions at low pressure given in Franklin and Snell (1998). So both limits are already well explored.

From (5), it is seen that $IU=X-e_2X^3/2+\ldots$, and in the limit $\delta_i\to 0$, e_2 can be shown to vary as

$$\frac{1}{N_0(N_0+1)\,(2N_0+1)}.$$

Thus $IU=X$ is a very good approximation at small δ_i and large N_0. On the other hand, at large δ_i,

$$X_w\,\delta_i^{1/2}\sim 1, \qquad e_2\sim\frac{1}{X_w^2}, \qquad IU\sim\sin X,$$

so that $IU\sim X-X^3/6+\ldots$, and $IU=X$ is a good approximation for $X\ll 1$. Thus it is to be expected that the positive-ion flux is nearly linear in all cases. That this is so can be seen from Fig. 4. Further examination of the equations for small X is given in Appendix B.

3.2. The boundary condition at the wall

Generally we require the negative-ion velocity W to be zero at the wall. In the case of the low-pressure magnetized column (Franklin and Snell 1999a), we found that the necessary additional boundary condition at the wall could be *either* $\Delta=0$, implying infinite spatial derivatives of densities and potential, or $E=0$, implying that the electron density was about to take on negative values – which is physically impossible. $E=0$ held generally at higher magnetic fields, i.e. equivalently higher pressures for the electrons.

In the present case, there is a similar situation, and if we take the limit δ_p, $\delta_n\to\infty$ then the value of Δ can be shown to be of one sign, since it then reduces to

$$\Delta=\frac{N}{\varepsilon_p}+\frac{I}{\varepsilon_n}+\frac{E}{\varepsilon_p\,\varepsilon_n},$$

and all the quantities involved are necessarily positive (or zero) and thus the boundary is then set by $N=I=E=0$.

https://doi.org/10.1017/S0022377800008576 Published online by Cambridge University Press

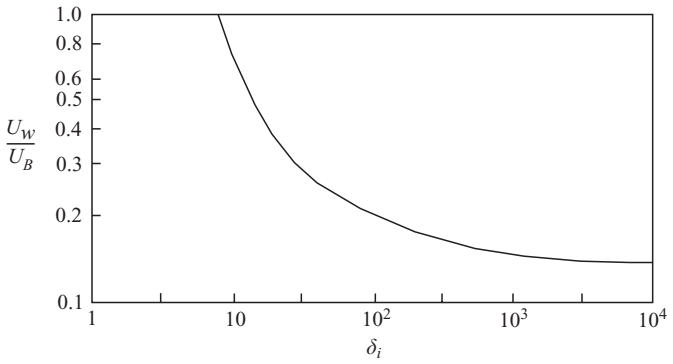


Figure 6. The ratio of the positive-ion speed at the boundary to the local Bohm speed given by (15) as a function of δ_i, for $N_0 = 3.0$, $\varepsilon_n = 100$ and $Q = 3$, showing that for $\delta_i > 10$ the Bohm speed is not reached within the plasma, and therefore the boundary condition must be changed.

On the other hand, as we noted above at (15), Δ has a zero where $U_B^2 = I/(E+\varepsilon_n N)$, and if this point is reached before the densities go to zero, it forms the boundary condition and is generally applicable at low pressure.

In order to further elucidate the boundary condition, we show in Fig. 6 the ratio of the positive-ion speed at the wall to the *local* generalized Bohm speed. The particular case chosen, which is typical, is for $N_0 = 3$, $Q = 1$ and $\epsilon_i = 100$. It can be seen that for $\delta_i \leqslant 10$ the ions reach this Bohm speed, but that for $\delta_i > 10$ they do not, and therefore the appropriate boundary condition is $N = 0$. It is of interest to compare this result with those given in Figs 2.9 and 4.7 of Franklin (1976), where it is evident that the transition from collisionless to collisional in *positive-ion–electron* plasmas is also characterized by $\delta_i \gtrsim 10$. Thus apparently the presence of negative ions – even when they are the dominant negative-charge carrier – does not alter the value of the parameter that characterizes the transition.

4. Recombination-dominated discharges

In recombination-dominated discharges, the positive-ion generation and loss is described by

$$\nabla\cdot(n_p\,\mathbf{v}_p) = Zn_e - \beta_e n_p n_e - \beta_i n_p n_n,$$

and the corresponding negative-ion equation is

$$\nabla\cdot(n_n\,\mathbf{v}_n) = An_e - \beta_i n_p n_n,$$

where β_e and β_i are the electron–positive-ion and positive-ion–negative-ion recombination coefficients. With the normalizations $\beta_e/\beta_i = H$ and $\beta_i n_{e0}/Z = J$, (5) and (7) are modified to

$$\frac{d}{dX}(IU) = E - JI(HE+N) \qquad (5'')$$

and

$$\frac{d}{dX}(NW) = PE - JIN. \qquad (7'')$$

https://doi.org/10.1017/S0022377800008576 Published online by Cambridge University Press

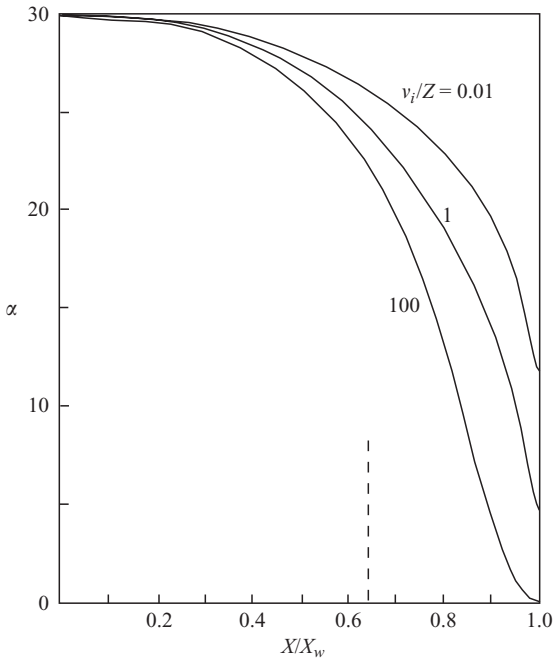


Figure 7. The variation of the negative-ion/electron density ratio α as a function of position X/X_w in a recombination-dominated plasma with parameters $N_0 = 30$, $P = A/Z = 0.424$, $J = \beta_i n_{e0}/Z = 7.11 \times 10^{-4}$ and $\varepsilon_n = 100$. The dashed line indicates the inner plasma core given by $X_0/X_w = P/J\alpha_0(\alpha_0 + 1)$.

Franklin et al. (1993) showed that in the collisional limit such discharges are necessarily structured, and that for high negative-ion concentrations there is a central core where $n_n = \alpha n_e$ is a good approximation surrounded by an essentially electron–positive-ion plasma where n_n is small. The analogue of (16) is

$$N_0 + P(N_0 + 1) = JN_0(N_0 + 1)\,(2N_0 + H + 1). \tag{17}$$

With the modifications to the right-hand side of (13) required by (5″) and (7″), we have solved those equations for a range of values of N_0, P and J, but have taken H to be zero.

The results indicate the same general features as found for attachment–detachment gases, and, in the core at higher pressures when $n_n \approx N_0 n_e$, the conclusion that $n_n \not\approx n_0 \exp(-\varepsilon\phi)$ is again reached. Figures 7–9 illustrate this point, with the parameters $N_0 = 30$, $Q = 0$, $H = 0$ and $J = 7.11 \times 10^{-4}$, corresponding to $P \approx 0.424$.

The general features found in recombination plasmas are similar to those already described in detachment plasmas but there are some important and subtle differences. First the attachment–ionization ratio P is necessarily less than 1, as was shown by Franklin et al. (1993). This has the consequence that the discharge has an ion–ion core surrounded by an essentially electron–ion plasma, but for reasonable temperature ratios, $\varepsilon_i \leqslant 100$, the boundary is not as sharp as for $\varepsilon_i \to \infty$, as was shown by Franklin and Snell (1994). It is also true that in the core $n_n/n_e = \text{const}$ is a less good approximation than in detachment plasmas. For this reason, the effective negative-ion temperature does not reach

https://doi.org/10.1017/S0022377800008576 Published online by Cambridge University Press

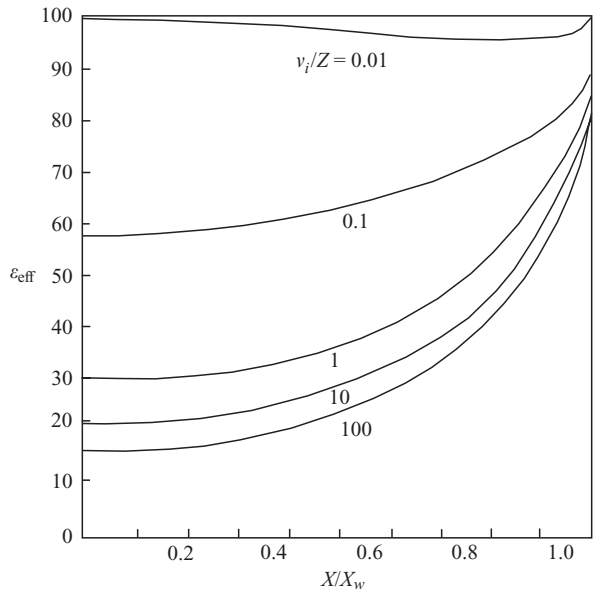


Figure 8. The variation of the effective temperature ratio $\varepsilon_{\text{eff}} = (1/\phi)\ln(N_0/N)$ in a discharge with the same parameters as in Fig. 7.

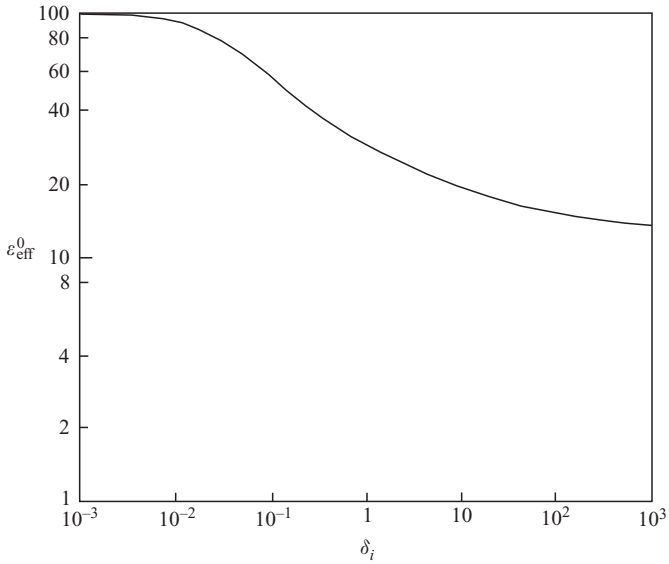


Figure 9. The variation of the central value of ε_{eff}, $\varepsilon^0_{\text{eff}}$, as a function of $\delta_i = \nu_i/Z$ for the same parameters as in Fig. 7.

the electron temperature, even at high collisionality. Figure 9 demonstrates this point. From (5″) and (7″), we have

$$\frac{d}{dX}(IU-NW) = E(1-P) \qquad \text{when} \quad H = 0.$$

Thus it is the electron flux, $\equiv IU-NW$, which is now closely linear with X,

https://doi.org/10.1017/S0022377800008576 Published online by Cambridge University Press

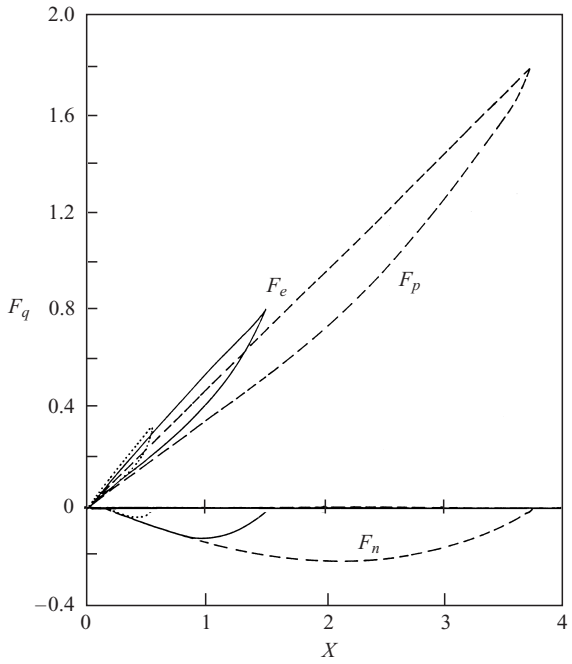


Figure 10. The normalized fluxes as functions of X. Dashed curves are for $\nu_i/Z = 0.01$, full curves for $\nu_i/Z = 1$ and dotted curves for $\nu_i/Z = 10$. The parameters are as in Fig. 7.

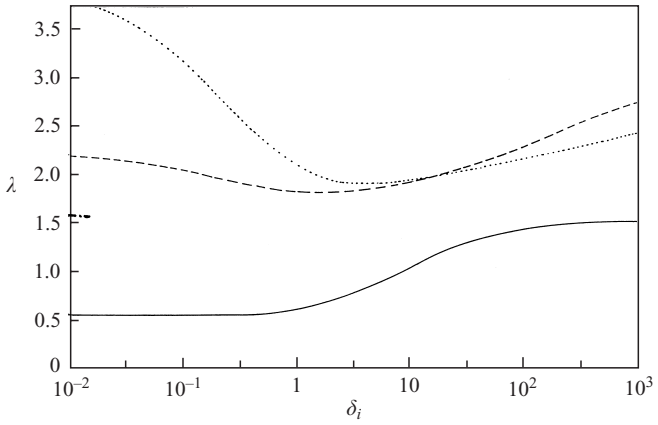


Figure 11. $\lambda = X_W(1+\delta_i)^{1/2}$ as a function of δ_i. The dashed curve is for $N_0 = 30$ and the other parameters of Fig. 2 (a detachment-dominated plasma). The dotted curve is for $N_0 = 30$ and the other parameters of Fig. 7 (a recombination-dominated plasma). For comparison, the solid curve is for the case where negative ions are absent, $N_0 = 0$.

rather than the positive-ion flux. This explains the differences between Figs 4 and 10, where Fig. 10 shows the fluxes for the recombination case.

We also show in Fig. 11 the variation of $\lambda = X_W(1+\delta_i)^{1/2}$ with δ_i for a detachment discharge (dashed) and a recombination discharge (dotted), both for $N_0 = 30$, and the equivalent variation for a conventional discharge $N_0 = 0$. The Schottky (1924) theory gives values for $\lambda \approx \frac{1}{2}\pi - 1 = 0.5708$ for $\nu_i \to 0$ and

https://doi.org/10.1017/S0022377800008576 Published online by Cambridge University Press

$\lambda \approx \frac{1}{2}\pi = 1.5708$ for $\nu_i \to \infty$. The value found by Franklin and Snell (1992) in the collisionless case ignoring negative-ion generation and loss for $N_0 = 30$ is shown as a line at the left-hand axis. It is of interest that there is a significant difference between the simple Boltzmann assumption and the inclusion of actual processes of generation and loss, and this will inevitably have consequences for the understanding of the oscillations observed under collisionless conditions (see Franklin 1999).

A simple model of an ion–ion core surrounded by an electron–ion plasma enables us to give estimates of λ that for the parameters of Fig. 11 for a detachment plasma, produce a large-δ_i limit of 3.23 and a minimum value of 2.0. These are consistent with the general form of the dashed curve. Furthermore, the recombination-dominated plasma produces similar results and in particular the same minimum value, which is again consistent with the dotted curve in Fig. 11.

5. Comparison with other work

The work referred to in Sec. 1 gave expressions for the particle ambipolar diffusion coefficients and the ambipolar electric field in the situation where there were negative ions of sufficient density to influence their values.

Given that the purpose of this paper is to obtain the correct expressions in the regime at higher pressures where $n_n = n_{n0} \exp(-\varepsilon_n \phi)$ is not a satisfactory description of the negative-ion density, we now set out the results appropriate to the situation where $n_n/n_e \approx \alpha$. This requires finding expressions for the coefficients D_{ap}, D_{ae} and D_{an} that relate the fluxes Γ_p, Γ_e and Γ_n and the particle gradients $\boldsymbol{\nabla} n_p$, $\boldsymbol{\nabla} n_e$ and $\boldsymbol{\nabla} n_n$. The results are given in Appendix A, but we shall give the results here and compare them with earlier work.

Figure 12 shows the variation of the effective diffusion coefficients with α, and Fig. 12 shows the variation of the electric field with α. They are apparently geometrically similar to those obtained by Thompson (1959), but closer inspection shows differences that cannot be ignored. First, at low α, the negative-ion coefficient is opposite in sign from the positive-ion and electron coefficients. For that reason, we have had to use a linear scale and not a logarithmic one in order to encompass the negative values. Secondly, the transition from negative-ion-free to negative-ion-dominated values of the various quantities occurs at values of α that differ by *orders of magnitude* from the treatment given here. In order to bring out this point, we also show in Fig. 13 the equivalent Thompson results.

Further, we examine the circumstances under which the two different treatments can be brought into harmony. Not surprisingly, we find that this requires $\varepsilon_i = 1$ in the Thompson treatment, but then it is further necessary to set $T_e = T_n = T_p$, which, although consistent with $\varepsilon_i = 1$, negates the physics of the situation that we are seeking to model. Thus we are driven to the conclusion that there is an inconsistency at the heart of Thompson's work, and that this lies in the use of the relationship $\boldsymbol{\nabla} n_n/n_n = \varepsilon_n \boldsymbol{\nabla} n_e/n_e$ at high pressures, when $n_n \approx \alpha_0 n_e$ is valid only under particular circumstances, and then $\nabla n_n/n_n = \boldsymbol{\nabla} n_e/n_e$.

Comparison with experimental work is possible in a few limited cases. The results given by Ferreira et al. (1988) and Gousset et al. (1991) are entirely

https://doi.org/10.1017/S0022377800008576 Published online by Cambridge University Press

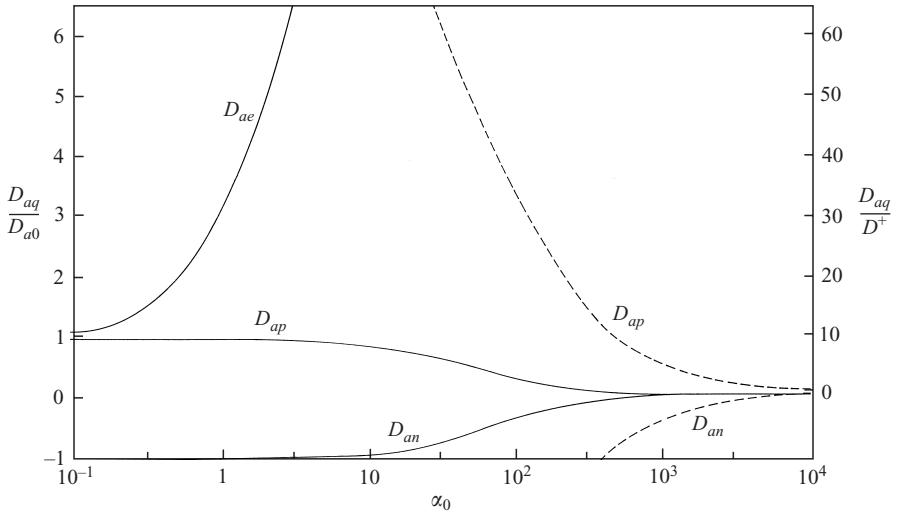


Figure 12. The ambipolar diffusion coefficients D_{ap}, D_{ae} and D_{an} for positive ions p, electrons e and negative ions n as functions of α_0 according to (A 7)–(A 9), normalized to their values in the absence of negative ions ($\alpha_0 = 0$). For large α_0, the ion ambipolar diffusion coefficients are also shown, normalized to the value when $\alpha_0 \to 0$ of the positive-ion diffusion coefficient D^+. The midpoint of the transition is $\alpha_0 \approx 50$, and the positive-ion value requires $\alpha_0 > 1000$. Here $\varepsilon_i = 100$ and $\mu_p = \mu_n = 10^{-2}\,\mu_e$.

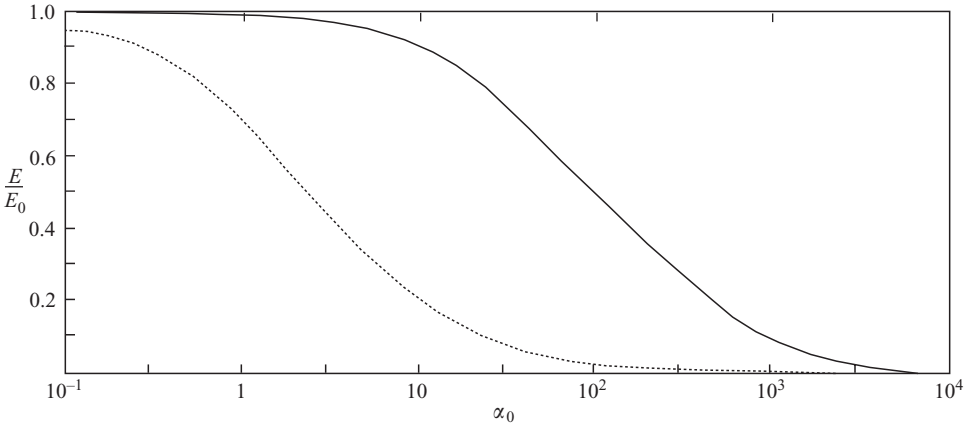


Figure 13. The full line shows the ambipolar field in an electronegative plasma according to (A 11), normalized to its value when $\alpha_0 = 0$, as a function of α_0. Again the midpoint of the transition is $\alpha_0 = 50$. The dashed line represents Thompson's expression obtained by setting $N = N_0 \exp(-\varepsilon_n \phi)$ for the same parameters as in Fig. 9.

consistent with the high-pressure limit described here for detachment-dominated discharges – in particular, the result that for $\alpha = \text{const}$, i.e. $P \gg 1$,

$$\varepsilon_{\text{eff}} \to 1 + \alpha \frac{\mu_n}{\mu_e} + (\alpha + 1)\frac{\mu_p}{\mu_e} \quad \text{for large } \delta_i,$$

as indicated in Fig. 3.

So far as recombination-dominated discharges are concerned, the most

https://doi.org/10.1017/S0022377800008576 Published online by Cambridge University Press

comprehensive measurements are those of Volynets et al. (1993) and Feoktistov et al. (1997), where it is shown that the discharge is structured with an ion–ion plasma core surrounded by an electron–ion plasma, and it is for this reason that there is no region where ε_{eff} is approximately constant. Volynets et al. in their computational work followed essentially the approach given above, but only for specific parameters related to their experiments.

6. Conclusions

The foregoing analysis allows a comprehensive description of plasmas dominated by negative ions, be they collisionless, collisional or transitional, albeit in the fluid approximation.

It has been shown that at higher pressures the negative ions should *not* be described by a Boltzmann distribution with the *negative-ion* temperature, but rather that in the regions where $n_n \approx \alpha n_e$ is a good approximation the negative ions are much closer to $n_n = n_{n0}\exp(eV/kT_e)$, i.e. a Boltzmann distribution characterized by the *electron* temperature.

Furthermore, combining $n_n = n_{n0}\exp(eV/kT_n)$ with $n_n \approx \alpha n_e$ leads to inconsistencies that cannot be justified when seeking to generate *ambipolar diffusion* coefficients for each of the three types of particle involved, because low-pressure and high-pressure limits are being used at the same time. Thus the proper expressions for these coefficients are derived and justified for higher pressures.

This removes an ambiguity that has existed in the literature for over 40 years, and solves the problem confronted, but not resolved, by Rogoff (1985). For this reason, we have given in Appendix A a detailed analysis leading to the correct expressions and the justification for them.

Thus we believe that we have answered in a definitive way the question posed in the title of this paper. Further, we believe that we have demonstrated that it is important to be able to justify any simplifying assumption made, albeit on physical grounds.

Appendix A

The conventional treatment of ambipolar diffusion is in terms of fluxes, diffusion coefficients and mobilities, and here we maintain that approach with $\Gamma_e = n_e v_e$, $\Gamma_p = n_p v_p$ and $\Gamma_n = n_n v_n$; the mobilities are $\mu_e e/m_e \nu_e$ and $\mu_p e/m_p \nu_p$; and the diffusion coefficients are $D_e = kT_e/m_e \nu_e$, $D_p = kT_p/m_p \nu_p$, $D_n = kT_n/m_n \nu_n$. Thus (3a, b, c) can be written as

$$\mathbf{\Gamma}_e = -D_e \nabla n_e - \mu_e \mathbf{E} n_e, \tag{A 1}$$

$$\mathbf{\Gamma}_p = -D_p \nabla n_p + \mu_p \mathbf{E} n_p, \tag{A 2}$$

$$\mathbf{\Gamma}_n = -D_n \nabla n_n - \mu_n \mathbf{E} n_n, \tag{A 3}$$

where $\mathbf{\Gamma}_e$, $\mathbf{\Gamma}_p$ and $\mathbf{\Gamma}_n$ are the physical fluxes and $\mathbf{E}$ is the electric field. Now $\Gamma_e + \Gamma_n = \Gamma_p$ and $n_e + n_n = n_p$, so that

$$\frac{n_e}{n_p} = \frac{1}{1+\alpha}, \qquad \frac{n_n}{n_p} = \frac{\alpha}{\alpha+1}, \tag{A 4}$$

https://doi.org/10.1017/S0022377800008576 Published online by Cambridge University Press

where $\alpha = n_n/n_e \equiv N/E$ (in terms of normalized densities). Expressing all the densities in terms of n_p from (A 4), we have

$$\mathbf{\Gamma}_p = \mathbf{\Gamma}_e + \mathbf{\Gamma}_n = \frac{-D_e \nabla n_p}{1+\alpha} - \frac{\alpha D_n}{1+\alpha}\nabla n_p - \left(\frac{\mu_e}{1+\alpha} + \frac{\mu_n \alpha}{1+\alpha}\right) n_p \mathbf{E}, \tag{A 5}$$

but, from (A 2),

$$\mathbf{\Gamma}_p = -D_p \nabla n_p + \mu_p n_p \mathbf{E}. \tag{A 6}$$

Eliminating $\mathbf{E}$ between (A 5) and (A 6) gives

$$\frac{\mu_e + \mu_n \alpha + \mu_p(1+\alpha)}{1+\alpha}\mathbf{\Gamma}_p = -\left[\frac{D_e + \alpha D_n}{1+\alpha}\mu_p + D_p\left(\frac{\mu_e}{1+\alpha} + \frac{\mu_n \alpha}{1+\alpha}\right)\right]\nabla n_p,$$

which rearranges to

$$\mathbf{\Gamma}_p = -D_{ap}\nabla n_p,$$

where

$$D_{ap} = \mu_p \frac{\mu_e(T_e+T_p) + \alpha\mu_n(T_n+T_p)}{\mu_e + \mu_p + \alpha(\mu_n+\mu_p)}\frac{k}{e}. \tag{A 7}$$

Similarly,

$$\mathbf{\Gamma}_e = -D_{ae}\nabla n_e, \qquad \mathbf{\Gamma}_n = -D_{an}\nabla n_n,$$

where

$$D_{ae} = \frac{\mu_n\mu_e\alpha(T_e - T_n) + (\alpha+1)\mu_p\mu_e(T_p+T_e)}{\mu_e + \alpha\mu_n + (\alpha+1)\mu_p}\frac{k}{e}, \tag{A 8}$$

$$D_{an} = \frac{\mu_e\mu_n(T_n - T_e) + (\alpha+1)\mu_p\mu_n(T_p+T_n)}{\mu_e + \alpha\mu_n + (\alpha+1)\mu_p}\frac{k}{e}. \tag{A 9}$$

The electric field

$$\mathbf{E} = -\frac{\nabla n_e}{n_e}\frac{D_e + \alpha D_n - (\alpha+1)D_p}{\mu_e + \alpha\mu_n + (\alpha+1)\mu_p}. \tag{A 10}$$

Since in general $D_e \gg D_n \sim D_p$ and n_e is monotonically decreasing, $\mathbf{E}$ is always of the same sign. And (A 10) leads directly to the result obtained by Kaganovich and Tsendin (1993) mentioned in Sec. 1.

The limiting values for small α are

$$D_{ap} = \mu_p\mu_e\frac{T_e+T_p}{\mu_e+\mu_p}\frac{k}{e}$$

$$\equiv D_{a0} \quad \text{(the classical ambipolar coefficient)},$$

$$D_{ae} = \mu_p\mu_e\frac{T_e+T_p}{\mu_e+\mu_p}\frac{k}{e} \equiv D_{a0} \approx \frac{\mu_p kT_e}{e},$$

$$D_{an} = \mu_n\left[\frac{\mu_p(T_n+T_n) - \mu_e(T_e - T_n)}{\mu_e+\mu_p}\right] \approx -\frac{\mu_n kT_e}{e}.$$

Thus Γ_n and Γ_p are opposite in sign for small α.

https://doi.org/10.1017/S0022377800008576 Published online by Cambridge University Press

For very large α, we have

$$D_{ap} \sim \frac{\mu_p \mu_n}{\mu_n + \mu_p}(T_n + T_p)\frac{k}{e}$$

which for $T_n = T_p = T_i$, $\mu_n = \mu_p = \mu_i$ becomes $\mu_i T_i \equiv D_i$, and

$$D_{ae} = \frac{\mu_n \mu_e (T_e - T_n) + \mu_p \mu_e (T_e + T_p)}{\mu_n + \mu_p}\frac{k}{e}$$

$$\to \frac{\mu_e k T_e}{e} = D_e \quad \text{(the free-electron value)}$$

and

$$D_{an} = \frac{\mu_p \mu_n (T_p + T_n)}{\mu_n + \mu_p}\frac{k}{e}$$

$$\to \frac{\mu_i k T_i}{e},$$

the same value as $D_{ap}(\infty)$.

The expressions obtained by Thompson (1959) and quoted by Massey (1974) and Lieberman and Lichtenberg (1994) agree with those given above for the positive-ion coefficient when $\alpha = 0$ and as $\alpha \to \infty$, but the transitions are separated by orders of magnitude. For the electron diffusion coefficient, they agree for all α, but only if $\mu_n = \mu_p = \mu_i$ and $D_n = D_p = D_i$; and for the negative-ion diffusion coefficient they only agree in the limit $\alpha \to \infty$. The fact that D_{an} is negative for $\alpha < (T_e - T_n)\mu_e/(T_p + T_n)\mu_p \approx 10^4$ is consistent with the negative values of Γ_n found by Edgley and von Engel (1980) and Ferreira et al. (1988).

So far as the electric field is concerned,

$$\frac{E(\alpha)}{E(0)} = \frac{D_e + \alpha D_n - (\alpha + 1)D_p}{\mu_e + \alpha \mu_n + (\alpha + 1)\mu_p}\frac{\mu_e + \mu_p}{D_e - D_p}, \tag{A 11}$$

which again is significantly different from the result of Thompson (1959) in that the transition values of α are

$$\alpha_1 = \frac{\mu_e + \mu_p}{\mu_n + \mu_p} \gg 1 \quad \text{and} \quad \alpha_2 = \frac{D_e - D_p}{D_n - D_p} \gg \alpha_1.$$

Note that if $D_n < D_p$ then, E may change sign. Thompson's transition values are 1 and $\sim \varepsilon_i$, i.e. two orders of magnitude smaller in α. As a further check, in (A 8) we put $e \to n$, $n \to e$ and $\alpha \to 1/\alpha$ to give

$$D_{an} = \frac{\mu_e \mu_n \dfrac{T_n - T_e}{\alpha} + \dfrac{\alpha + 1}{\alpha}\mu_p \mu_n (T_p + T_n)}{\mu_n + \dfrac{1}{\alpha}\mu_e + \dfrac{\alpha + 1}{\alpha}\mu_p}$$

$$= \frac{\mu_e \mu_n (T_n - T_e) + (\alpha + 1)\mu_p \mu_n (T_p + T_n)}{\mu_e + \alpha \mu_n + (\alpha + 1)\mu_p},$$

$$\equiv \text{(A 9)},$$

https://doi.org/10.1017/S0022377800008576 Published online by Cambridge University Press

and, for the field $\mathbf{E}$ as defined in (A 10),

$$\mathbf{E} = -\frac{\boldsymbol{\nabla} n_n}{n_n}\frac{D_n+\frac{1}{\alpha}D_e-\frac{\alpha+1}{\alpha}D_p}{\mu_n+\frac{1}{\alpha}\mu_e+\frac{\alpha+1}{\alpha}\mu_p}$$

$$= -\frac{\boldsymbol{\nabla} n_n}{n_n}\frac{D_e+\alpha D_n-(\alpha+1)D_p}{\mu_e+\alpha\mu_n+(\alpha+1)\mu_p},$$

$$\equiv \text{(A 10)}, \quad \text{since} \quad \frac{\boldsymbol{\nabla} n_e}{n_e} = \frac{\boldsymbol{\nabla} n_n}{n_n}.$$

As a final check on (A 8) and (A 9), we put $T_e = T_n = T^-$ and $\mu_e = \mu_n = \mu^-$ thus making the two types of negative particle identical, giving, for both D_{an} and D_{ae},

$$D_a^- = \frac{\mu_p\mu^-(T^-+T_p)}{\mu^-+\mu_p},$$

independent of α, as it should be, and identical to (A 7) when $T_e = T_n = T^-$ and $\mu_e = \mu_n = \mu^-$, again as it should be.

For small α, we can expand the fluxes in powers of α, and likewise the D_{aq}, so that

$$\boldsymbol{\Gamma}_p \equiv \boldsymbol{\Gamma}_{p0}+\alpha\boldsymbol{\Gamma}_{p1}+\alpha^2\boldsymbol{\Gamma}_{p2}+\ldots = -(D_{ap0}+\alpha D_{ap1}+\ldots)\boldsymbol{\nabla} n_p \qquad \text{(A 12)}$$

and

$$\boldsymbol{\Gamma}_e \equiv \boldsymbol{\Gamma}_{e0}+\alpha\boldsymbol{\Gamma}_{e1}+\alpha^2\boldsymbol{\Gamma}_{e2}+\ldots = \frac{-(D_{ae0}+\alpha D_{ae1}+\ldots)\boldsymbol{\nabla} n_p}{1+\alpha}. \qquad \text{(A 13)}$$

Then

$$\boldsymbol{\Gamma}_n \equiv \boldsymbol{\Gamma}_{n0}+\alpha\boldsymbol{\Gamma}_{n1}+\alpha^2\boldsymbol{\Gamma}_{n2}+\ldots = \frac{-\alpha(D_{an0}+\alpha D_{an1}+\ldots)\boldsymbol{\nabla} n_p}{1+\alpha} \qquad \text{(A 14)}$$

But $\boldsymbol{\Gamma}_p = \boldsymbol{\Gamma}_e+\boldsymbol{\Gamma}_n$ and, from (A 14), $\boldsymbol{\Gamma}_{n0} = 0$, so that

$$\boldsymbol{\Gamma}_{p0} = \boldsymbol{\Gamma}_{e0} = \frac{-\mu_e\mu_p(T_e+T_p)}{\mu_e+\mu_p}\boldsymbol{\nabla} n_p,$$

using (A 7) and (A 8). To *first* order in α, we have, $\boldsymbol{\Gamma}_{p1} = \boldsymbol{\Gamma}_{e1}+\boldsymbol{\Gamma}_{n1}$, or $D_{ap1} = D_{ae1}-D_{ae0}+D_{an0}$, giving

$$D_{an0} = -D_{ae1}+D_{ap1}+D_{ae0}, \qquad \text{(A 15)}$$

or

$$\frac{\mu_e\mu_n(T_n-T_e)+\mu_p\mu_n(T_p+T_n)}{\mu_e+\mu_p} = \frac{\mu_e\mu_p(T_e+T_p)}{\mu_e+\mu_p}\left[\frac{\mu_n(T_n-T_e)}{\mu_p(T_e+T_p)}+\frac{\mu_n(T_n+T_p)}{\mu_e(T_e+T_p)}\right],$$

using (A 7)–(A 9). Since this is an identity, we have verified the validity of (A 7) and (A 8) to first order in α and (A 9) to zeroth order.

The value of (A 15), $D_{an0}+D_{ae1}-D_{ap1}-D_{ae0}$, using Thompson's expressions, is

$$\frac{(\varepsilon_i-1)(\varepsilon_i+1)}{\mu_e+\mu_p}\left(\mu_e-\frac{\mu_n}{\varepsilon_i}\right)D_p,$$

https://doi.org/10.1017/S0022377800008576 Published online by Cambridge University Press

i.e. it is zero if $\varepsilon_i = 1$, but not otherwise. And putting $\varepsilon_i = 1$ is equivalent to setting $\nabla n_e/n_e = \nabla n_n/n_n$ rather than $\nabla n_n/n_n = \varepsilon_n \nabla n_e/n_e$; so once again we conclude that $\nabla n_n/n_n = \varepsilon_n \nabla n_e/n_e$ is not valid in these circumstances.

Thus we are led to examine the expressions given by Thompson under the condition $\varepsilon_i = 1$. Then

$$D_a^+ = 2D^+\left[\frac{1+\alpha\,\mu_n/\mu_e}{1+\alpha\,\mu_n/\mu_e+(1+\alpha)\,\mu_p/\mu_e}\right],$$

$$D_a^- = 2D^+\left[\frac{\mu_n}{\mu_e}\,\frac{1+\alpha}{1+\alpha\,\mu_n/\mu_e+(1+\alpha)\,\mu_p/\mu_e}\right],$$

$$D_a^e = 2D^+\left[\frac{1+\alpha}{1+\alpha\,\mu_n/\mu_e+(1+\alpha)\,\mu_p/\mu_e}\right].$$

With $T_n = T_p = T^+$, then,

$$D_a^+ = \mu^+\,\frac{\mu_e(2T^+)+\alpha\mu_n(2T^+)}{\mu_e+\alpha\mu_n+(1+\alpha)\,\mu_p},$$

$$D_a^- = \mu^+\,\frac{2\mu_n(1+\alpha)\,T^+}{\mu_e+\alpha\mu_n+(1+\alpha)\,\mu_p},$$

$$D_a^e = \mu^+\,\frac{2\mu_e\,T^+(1+\alpha)}{\mu_e+\alpha\mu_n+(1+\alpha)\,\mu_p}.$$

These expressions are now similar to (A 7)–(A 9), and would be identical if, and only if, $T_e = T_n = T_p = T^+$, which is consistent with $\varepsilon_i = 1$.

So we have managed to show the 'equivalence' of the two treatments and that they are identical *if* all the temperatures are set equal – but that is beside the point. The normalized gradients *are* equal, $\nabla n_e/n_e = \nabla n_n/n_n = \nabla n_p/n_p$, but the corresponding temperatures *are not*, and that is the nub of the issue. We conclude that (A 7)–(A 9) are the correct expressions when it is permissible to put $n_n/n_e = \alpha$, where α is a constant or nearly so.

Appendix B

Here we examine in greater detail the structure of the solutions near the centre of the plasma, that is for small values of X, and we take the ion temperatures to be small compared with the electron temperature. Accordingly, we return to (4′), (6′) and (8′), and examine the values of e_2, n_2 and f_2 as δ_p and δ_n vary.

To reduce the algebraic complexity, we set $\delta_p = \delta_n = \delta_i$, and $1/\varepsilon_p = 1/\varepsilon_n = \tau$, and set $\delta_e/\delta_i = \rho$. The equations to be solved are

$$-e_2+\tfrac{1}{2}\rho\delta_i[1-P+QN_0]+f_2 = 0, \tag{B 1}$$

$$\frac{1}{N_0+1}-n_2\tau-e_2\tau+\tfrac{1}{2}\delta_i-(N_0+1)f_2 = 0, \tag{B 2}$$

$$\frac{(P-QN_0)^2}{N_0}-n_2\tau+\tfrac{1}{2}\delta_i(P-QN_0)+N_0f_s = 0. \tag{B 3}$$

https://doi.org/10.1017/S0022377800008576 Published online by Cambridge University Press

In the limit $\tau \to 0$ and $\delta_i \to \infty$, for (B 2) and (B 3) to be consistent, $N_0 + (P - QN_0)(N_0 + 1) = 0$, as already noted.

Taking $\rho = 0$, (B 1) becomes $e_2 = f_2$, and, using the result from Ferreira et al. (1988) that $N/E = N_0$ for $P, Q \gg 1$, $E = 1 - e_2 X^2$, $N = N_0 - n_2 X^2 \equiv N_0(1 - e_2 X^2)$ or $N_2 = N_0 e_2$, gives, for (B 2) and (B 3),

$$\frac{1}{N_0 + 1} + \tfrac{1}{2}\delta_i - (N_0 \tau + \tau + N_0 + 1) f_2 = 0, \tag{B 4}$$

$$\frac{(P - QN_0)^2}{N_0} + \tfrac{1}{2}\delta_i (P - QN_0) + N_0(1 - \tau) f_2 = 0. \tag{B 5}$$

Equation (B 4) gives f_2, and the requirement for consistency for large δ_i leads to the generalization

$$QN_0(N_0 + 1) = P(N_0 + 1) + N_0 \frac{1 - \tau}{1 + \tau}. \tag{B 6}$$

The corresponding result with $\rho \neq 0$ is

$$QN_0(N_0 + 1) = P(N_0 + 1) + N_0 \frac{1 - \tau[1 + 2\rho(N_0 + 1)]}{1 + \tau(1 + 2\rho N_0)},$$

and, for recombination discharges,

$$\frac{JN_0(N_0 + 1)\,(2N_0 + \tau + 1)}{1 + \tau(1 + 2\rho N_0)} = P(N_0 + 1) + N_0 \frac{1 - \tau[1 + 2\rho(N_0 + 1)]}{1 + \tau(1 + 2\rho N_0)}.$$

Setting $QN_0 - P = G$ in (B 4) and (B 5) and solving the relevant quadratic for large ε_i, one finds that to first order in δ_i^{-1},

$$G \approx \left[1 + \frac{2}{\delta_i (N_0 + 1)}\right] \frac{N_0}{N_0 + 1} \frac{1 - \tau}{1 + \tau}. \tag{B 7}$$

We now return to (B 1) and substitute for G:

$$e_2 \approx f_2 + \frac{\delta_i \rho}{2}\left[1 - \frac{N_0(1 - \tau)}{(N_0 + 1)\,(1 + \tau)}\right] = f_2 + \delta_i \rho \left[\frac{N_0 \tau + \tfrac{1}{2}(1 + \tau)}{(N_0 + 1)\,(1 + \tau)}\right]. \tag{B 8}$$

Typically, ρ is 10^{-2} and τ is 10^{-2}, so that, for values of $N_0 < 100$, the correction to f_2 is less than 1 %. Thus $e_2 \approx f_2$ is a good approximation for all δ_i.

At low pressures, (B 1) becomes $e_2 = f_2$ and (B 2) approximately

$$f_2 = \frac{1}{(N_0 + 1)\,(2N_0 + 1)},$$

while (B 3) gives $n_2 = N_0 f_2 \varepsilon$.

The next highest order in δ_i is given by

$$f_2(N_0 + 1 + \tau + N_0) = \frac{1}{N_0 + 1} + \tfrac{1}{2}\delta_i \tag{B 9}$$

and

$$n_2 = \varepsilon \left[N_0 f_2 + \tfrac{1}{2}\delta_i (P - QN_0) + \frac{(P - QN_0)^2}{N_0}\right]. \tag{B 10}$$

https://doi.org/10.1017/S0022377800008576 Published online by Cambridge University Press

We conclude that the transition from low-pressure to high-pressure behaviour begins at $\delta_i \approx 1/(N_0+1)$.

We note that we cannot simply put $\delta_i = 0$ and have (B 2) and (B 3) consistent, because that would require

$$\frac{N_0}{(N_0+1)\,(P-QN_0)^2} = \frac{1}{1} = \frac{-(N_0+1+\tau)}{N_0}, \quad \text{or} \quad 2N_0+1+\tau = 0,$$

and

$$(P-QN_0)^2\,(N_0+1)\,(N_0+1+\tau)+N_0^2 = 0.$$

Physically,

$$\delta_i = \frac{\nu_i}{Z} = \frac{\nu_i/p}{Z/p};$$

the numerator is approximately constant while the denominator becomes large at low pressure p because $Z/p = (Z/p)\,(T_e)$ and T_e is large; likewise, $P = A/Z$ and $Q = D/Z$ behave similarly at low p. Thus the correction to n_2 represented by the second and third terms on the right-hand side of (B 10) is of second order in δ_i.

Appendix C

The basic equations (13) that we have solved for both detachment and recombination discharges can be written formally as

$$\begin{pmatrix} \lambda & -I & 0 \\ 0 & N & \mu \\ 1 & E & -1 \end{pmatrix} \begin{pmatrix} dI/dX \\ d\phi/dX \\ dN/dX \end{pmatrix} = \begin{pmatrix} \rho_1 \\ \rho_2 \\ \rho_3 \end{pmatrix}, \tag{C 1}$$

where

$$\lambda = \frac{1}{\varepsilon_\rho} - U^2, \qquad \mu = \frac{1}{\varepsilon_n} - W^2$$

and the determinant

$$\Delta = -(I\mu + N\lambda + E\lambda\mu). \tag{C 2}$$

In general, inverting (C 1), we have

$$\Delta \frac{dI}{dX} = -\rho_1(N+\mu E) - \rho_2 I - \rho_3 \mu I, \tag{C 3}$$

$$\Delta \frac{d\phi}{dX} = -\rho_1 \mu + \rho_2 \lambda + \rho_3 \lambda\mu, \tag{C 4}$$

$$\Delta \frac{dN}{dX} = -\rho_1 N_1 - \rho_2(\lambda E + I) + \rho_3 \lambda N. \tag{C 5}$$

But, at low pressures, typically $\nu_i/Z \leqslant 10$, the appropriate boundary conditions at the plasma edge are $\Delta = 0$ and $W = 0$. Thus, using (C 2) 'at the plasma edge',

$$\frac{\Delta}{I}\frac{dI}{dX} = \rho_1 \mu - \rho_2 \lambda - \rho_3 \lambda\mu, \tag{C 6}$$

https://doi.org/10.1017/S0022377800008576 Published online by Cambridge University Press

$$\Delta \frac{d\phi}{dX} = -\rho_1 \mu + \rho_2 \lambda + \rho_3 \lambda \mu, \tag{C 7}$$

$$\mu \frac{\Delta}{N} \frac{dN}{dX} = \rho_1 \mu - \rho_2 \lambda - \rho_3 \lambda \mu. \tag{C 8}$$

Apart from sign, the right-hand sides of (C 6)–(C 8) are identical and allow us to deduce, dividing (C 6) by (C 7) and (C 8) by (C 7), that, at the boundary, $E \sim \exp(-\phi)$ and $N \sim \exp(-\varepsilon_n \phi)$, since when $W = 0, \mu = 1/\varepsilon_n$. This explains the rising right-hand portion of Fig. 2, and demonstrates that the local value of ε_{eff}, $\varepsilon^l_{\text{eff}} \equiv \varepsilon_n$ at the boundary.

References

Daniels, P. G., Franklin, R. N. and Snell, J. 1990 *J. Phys. D: Appl. Phys.* **23**, 823–831.

Edgley, P. D. 1975 DPhil Thesis, Oxford University.

Edgley, P. D. and von Engel, A. 1980 *Proc. R. Soc. Lond.* **A370**, 375–387.

Feoktistov, V. A., Ivanov, V. V., Opov, A. M., Rakhimov, A. T., Rakhimova, T. V., Slovetsky, D. I. and Volynets, V. N. 1997 *J. Phys. D: Appl. Phys.* **30**, 423–431.

Ferreira, C. M., Gousset, G. and Touzeau, M. 1988 *J. Phys. D: Appl. Phys.* **21**, 1403–1413.

Forrest, J. R. and Franklin, R. N. 1966 *Br. J. Appl. Phys.* **17**, 1569–1578.

Franklin, R. N. 1976 *Plasma Phenomena in Gas Discharges*. Oxford University Press.

Franklin, R. N. 1999 *J. Phys. D: Appl. Phys.* **32**, L71–L74.

Franklin, R. N. and Snell, J. 1992 *J. Phys. D: Appl. Phys.* **25**, 453–457.

Franklin, R. N. and Snell, J. 1994 *J. Phys. D: Appl. Phys.* **27**, 2102–2106.

Franklin, R. N. and Snell, J. 1998 *J. Phys. D: Appl. Phys.* **31**, 2532–2542.

Franklin, R. N. and Snell, J. 1999a *J. Phys. D: Appl. Phys.* **32**, 1031–1038.

Franklin, R. N. and Snell, J. 1999b *J. Phys. D: Appl. Phys.* **32**, 2190–2203.

Franklin, R. N., Daniels, P. G. and Snell, J. 1993 *J. Phys. D: Appl. Phys.* **26**, 1638–1649.

Gousset, G., Ferreira, C. M., Pinheiro, M., Sá, P. A., Touzeau, M., Vialle, M. and Loureiro, J. 1991 *J. Phys. D: Appl. Phys.* **24**, 290–300.

Kaganovich, I. D. and Tsendin, L. D. 1993 *Plasma Phys. Rep.* **19**, 645–650.

Lieberman, M. A. and Lichtenberg, A. J. 1994 *Principles of Plasma Discharges and Materials Processing*. Wiley-Interscience, New York.

Massey, H. S. W. 1976 *Negative Ions*, pp. 645–648. Cambridge University Press.

Riemann, K.-U. 1995 *IEEE Trans. Plasma Sci.* **23**, 709–716.

Rogoff, G. L. 1985 *J. Phys. D: Appl. Phys.* **18**, 1533–1545.

Schottky, W. 1924 *Phys. Z.* **25**, 635–639.

Thompson, J. B. 1959 *Proc. Phys. Soc.* **73**, 818–821.

Tsendin, L. D. 1989 *Soviet Phys. Tech. Phys.* **34**, 11–15.

Valentini, H. B. and Herrmann, F. 1996 *J. Phys. D: Appl. Phys.* **29**, 1175–1180.

Volynets, V. N., Lukyanova, A. V., Rakhimov, A. T., Slovetsky, D. I. and Suetin, N. V. 1993 *J. Phys. D: Appl. Phys.* **26**, 647–656.

https://doi.org/10.1017/S0022377800008576 Published online by Cambridge University Press